FY2013 Theory Milestone
Fourth Quarterly Report
September 30, 2013

Submitted by: S. C. Jardin, PPPL jardin@pppl.gov

I. Introduction and Outline

The FY2013 Theory Target on Disruption Physics consists of two major topics which we will refer to as "disruption forces" and "runaway electron confinement during MGI".   Both of these have several sub-topics. The Q1 quarterly report concerned only disruption forces, and the Q2 report concerned only runaway electron confinement during MGI.   The original plan was to continue this separation with the Q3 and Q4 reports each being a report on only one of these two topics. However, as explained in the Q3 report, in Q3 we presented a progress report on both the original Q3 and Q4 milestones, as listed in the Appendix.   This final Q4 report contains the final analysis of both topics, thus successfully completing the FY2013 Theory Target.

II. Calculation of Disruption Forces in ITER

In the simulations presented in this section, we used a poloidal computational mesh with 43,200 points and 32 toroidal planes.   This is a total of 1,382,400 mesh points.   This mesh is the same as used in Q3, and is 2^3 times larger than those used in the previous ITER simulations reported in Q1.   This increased resolution allows the use of more realistic parameters.   In particular, the Lundquist number is S = 10^6, and the resistive wall penetration time is much greater than the Alfven time, $\tau_{wall} = 10^4 \tau_A$. **The timescales of the disruption are much better separated than in previous work.**

Our simulations modeled asymmetric vertical displacement event (AVDE) disruptions, which are expected to be the worst case scenario for plasma wall interaction and generation of electromechanical forces on the walls and surrounding structures in ITER. We emphasized calculation of the toroidally asymmetric wall force F_x which is the most difficult force to compensate mechanically.

Our main finding was that the expected asymmetric wall force F_x is less than 10% of the maximum tolerable by the ITER wall and mechanical stuctures. Another finding is that the force F_x rotates toroidally. Near the end of the current quench, the rotation frequency is possibly resonant with the ITER structure.

An AVDE disruption has three timescales. The first timescale is the vertical displacement event (VDE) growth time , which is the resistive wall penetration time, τ_{wall} . The VDE scrapes off magnetic flux, causing the safety factor, q, at the last closed flux surface to drop to $q \cong 2$, causing the plasma to become ideal MHD unstable.

The second time scale is the thermal quench (TQ) time, which depends on the growth time of toroidally asymmetric $n=1$ modes, denoted by γ^{-1} .   These modes, with poloidal and toroidal mode numbers

(m,n) predominantly (2,1) and (1,1), cause the magnetic field to become stochastic, producing the TQ, which drastically cools the plasma to the halo temperature. Hence $\tau_{TQ} = \gamma^{-1}$.

The third timescale is the current quench (CQ) time. It is primarily determined by the external circuit inductance, and also by the halo resistivity, which is also the bulk plasma resistivity after the TQ. Note that the resistive time of the pre-thermal quench plasma, $\tau_r = S \, \tau_A$ is not important, as long as it is large enough not to have much effect on γ. The S value of the halo in the following was $S_{halo}=10^3$. In previous work, the external circuit was not included in the simulation. Without it, the TQ and CQ coincide. Using a model current controller permits temporal separation of the TQ and CQ.

In previous work [1,2], we found the asymmetric wall force F_x was maximum when $\gamma\tau_{wall} \approx 1$ (Note that $\gamma \approx 0.01\tau_A^{-1}$) This is shown in Fig. 1. Realistically, $\gamma\tau_{wall} \gg 1$, so that the asymmetric wall force F_x should be much smaller than its maximum value.
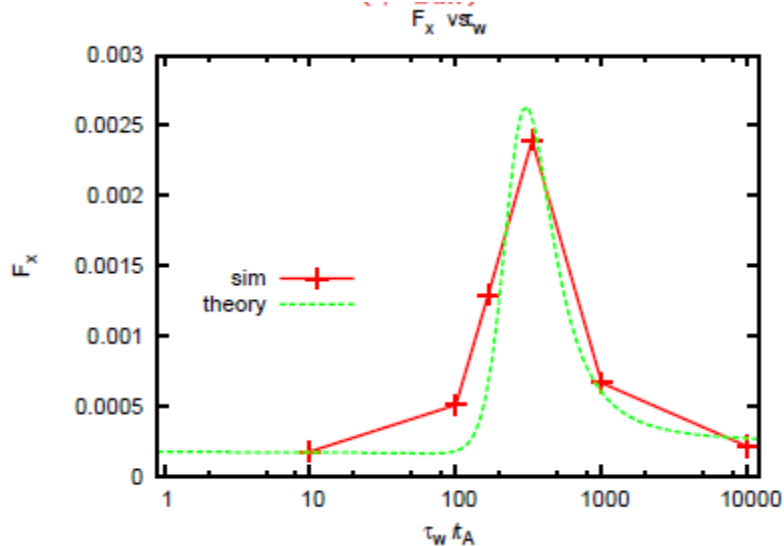

Figure 1: Previous calculations [1,2] showed the relation between the asymmetric wall force and the wall time.

The reason for the dependence $F_x(\gamma\tau_{wall})$ was explained in Ref. [2]. The maximum wall force is only obtained when the VDE and n=1 modes saturate at the same time. Consistent with Fig. 1, we find in Fig. 3 that the maximum asymmetric wall force F_x is only 5% of the maximum tolerable by ITER. This is a very important self mitigating effect for ITER disruptions.
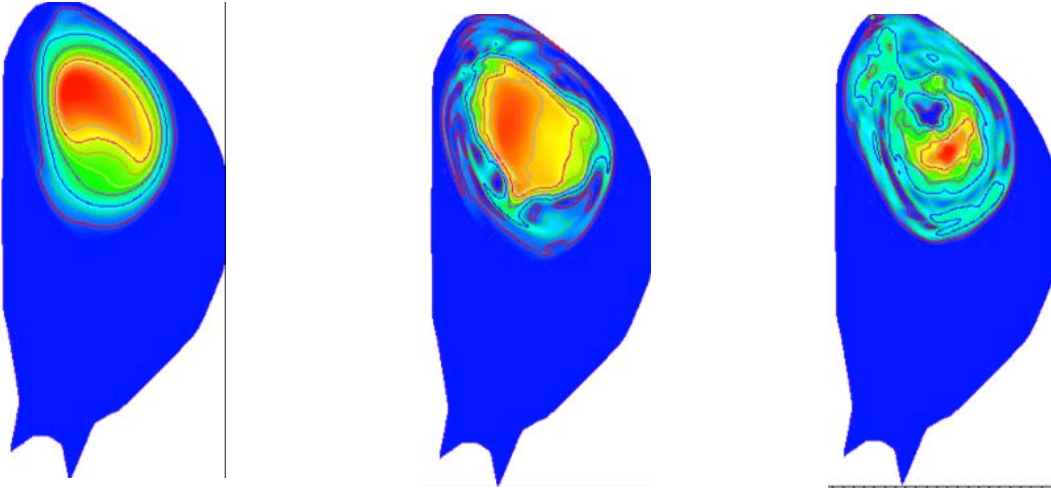
Figure 2: Contour plots of *p(R,Z,0)* at times t = 700, 907, and 1035 τ_A. The pressure perturbations are dominated by (2,1) and (1,1) modes, which overlap with each other and with other modes to break up magnetic surfaces and pressure surfaces.

Figure 2 shows a snapshot of the pressure contours in a high resolution simulation at times t = 700, 907, and 1035 τ_A. The parameters are S = 10^6, $\tau_{wall} = 10^4 \tau_A$ and $S_{halo} = 10^3$. The nonlinear perturbed pressure at t = 700 τ_A shows that the perturbations are dominated by (m,n) = (2,1) and (1,1) modes. At the later time t = 907 τ_A the plasma shows evidence of stochastic breakup of pressure surfaces, which involves the entire plasma at t= 1035 τ_A.
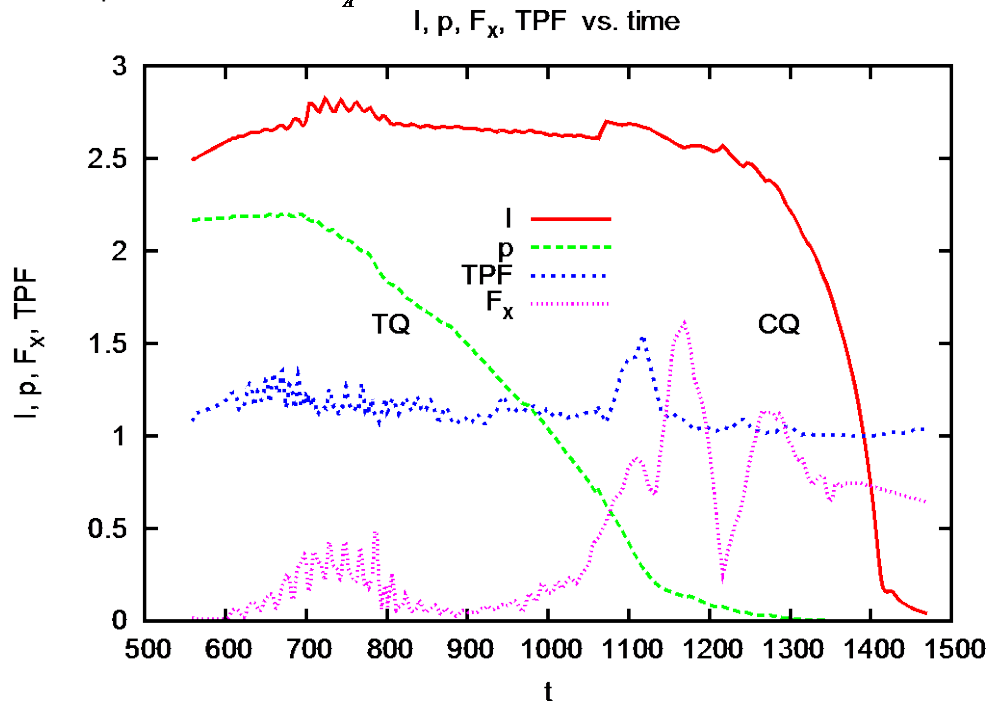

Figure 3: Time history of milestone simulation

Figure 3 shows traces for the time history of the simulation shown in Figure 2. Shown are normalized total current I, normalized total pressure p , toroidal peaking factor (TPF), and F_x ,the dimensionless sideways wall force multiplied by 10^4.   Here **the maximum value of F_x is only 5% of that which can be tolerated by ITER**.

During the CQ, there are a few low frequency oscillations of the sideways force F_x . There are also smaller, higher frequency oscillations during the TQ. The cause is evidently sheared toroidal rotation induced by MHD instability [3]. It may be a concern for ITER that the oscillations might resonate with the ITER vacuum vessel and other mechanical structures.

The current controller, which models external circuit inductance, caused the CQ to be delayed after the TQ. The separation of TQ and CQ time scales in Fig. 3 makes it clear that the peak sideways force is produced during the CQ rather than the TQ. The initial increase of the plasma current I is caused by a modification of the resistivity profile and subsequent change in the internal inductance in the initial stage of the simulation.

To summarize, the milestone simulation of asymmetric wall force in an AVDE improved greatly on previous simulations [1],[2], with higher resolution, and especially with much better time separation of the three phases of the AVDE: the VDE, TQ, and CQ. The simulations confirmed that the sideways force predicted in ITER is much less than the maximum tolerable force, because in ITER it is expected that $\gamma \tau_{wall} \gg 1$, at least for disruptions involving ideal MHD kink modes. It is conceivable that the situation could be different for resistive wall modes which have $\gamma \tau_{wall} \approx 1$.   This should be investigated further.

Another finding is that the force F_x rotates toroidally. Near the end of the current quench, the rotation frequency is possibly resonant with the ITER structures. These questions will be investigated in future work.

III. Runaway electron confinement with spatially non-symmetric source terms: MHD mode spectra for HFS vs. LFS MGI

The non-linear evolution of the n=1 mode for six massive-gas-injection (MGI) simulations was presented in the Q3 milestone report, along with the loss fraction of runaway electron (RE) test particles. For both toroidally symmetric and toroidally localized gas injection on the low-field-side (LFS) of the tokamak, it was observed that the period of rapid RE loss coincided with the saturation of the n=1 mode. For the case of high-field-side (HFS) injection, not only were REs more effectively de-confined, but the losses were seen to precede the saturation of the n=1 mode. To understand the HFS injection results, we now consider the complete MHD mode spectra for four cases—two with HFS injection and two with LFS injection (Fig. 4). For each poloidal injection profile the two cases differ according to the extent of toroidal Ne distribution, with the Ne spread about 2/3 of the way around in one case and only 1/3 in the other case.
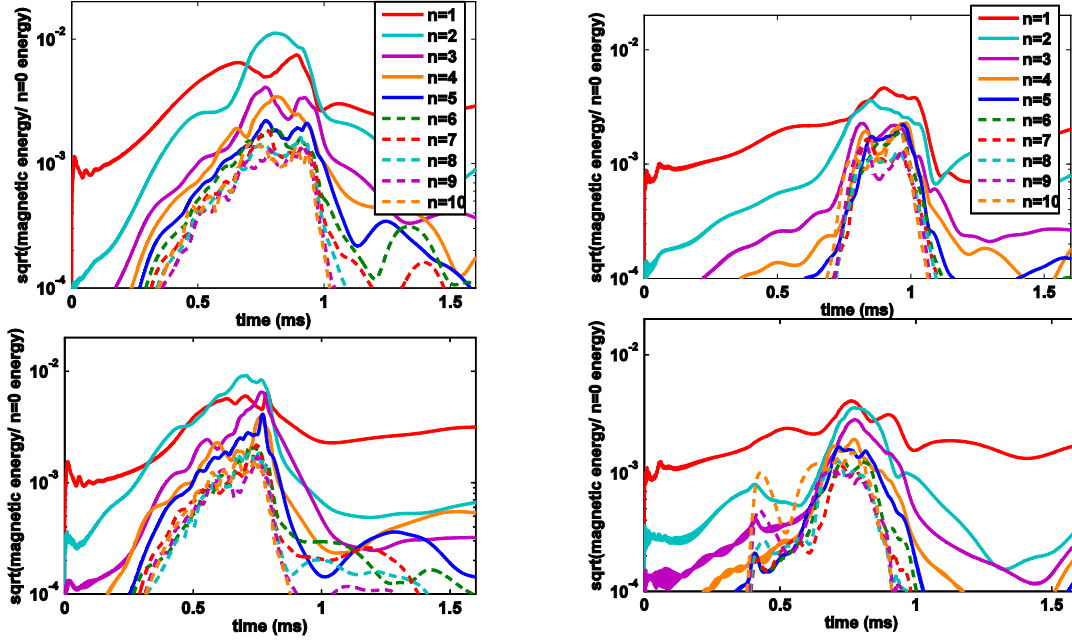
Figure 4. Evolution of magnetic energy (in units of $\delta B/B$) for all n>0 modes for four simulations. (Left column) HFS injection; (Right column) LFS injection. (Upper row) 2/3 toroidal spreading of Ne source; (Lower row) 1/3 toroidal spreading.

The fact that the n=2 mode reaches the largest amplitude in both HFS injection cases is in contrast to all simulations with LFS injection. But, the time at which the n=2 mode reaches its peak is well after the RE losses occur. However, faster growth of the n=2 mode is also seen at earlier times in the HFS cases, so that even by 0.5 ms, the n=2 amplitude is well above 10^{-3} for both HFS cases. The large initial amplitude of the n=1 magnetic energy in these simulations is due to the global n=1 perturbation from the gas jet, and not the growth of an unstable internal mode. But, the standard picture in which a 2/1 mode is first destabilized in the sequence leading to the eventual core thermal quench holds in these simulations. In fact, in the HFS cases, the n=2 mode is also a q=2 mode, with a dominant 4/2 structure at early times. This can be seen in a plot (Figure 5) of the n=1 and n=2 parts of the toroidal current density at 0.3 ms for the case plotted
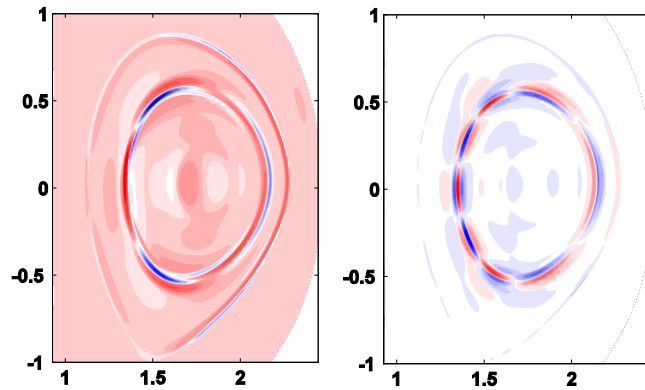

Figure 5: Toroidal current density at 0.3 ms for a HFS simulation. (Left)The n=1 part showing the large global perturbation from the jet, plus the dominant growing 2/1 mode. (Right) The n=2 part showing the 4/2 structure of the n=2 mode.

in the lower left above.

Since stochastization requires island overlap, the spacing of the integer q-rational surfaces will generally require a very large n=1 amplitude or the appearance of other modes before this occurs. The faster early time growth of the n=2 mode (and indeed the n>2 modes, which are also initially q=2 modes) with HFS injection leads to earlier flux surface destruction and therefore RE losses. This can be seen in a comparison of the two simulations from the upper row of Fig. 4, both at 0.4 ms, where the LFS injection case has large but discrete n=1 islands, and the HFS case has a stochastic region at the edge (Fig. 6).
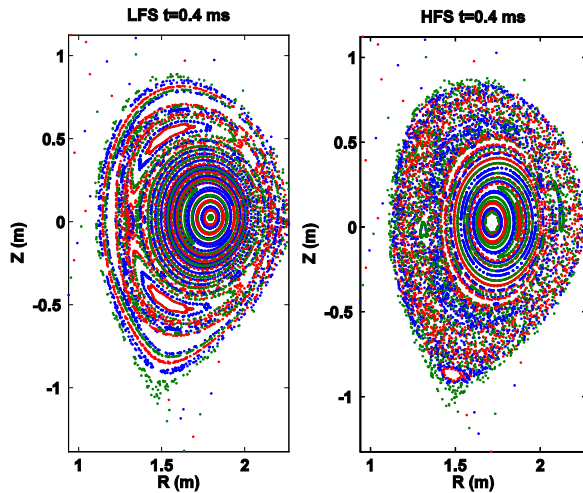

Only one particular HFS peaked and one LFS peaked injection profile have been considered (although with varying toroidal localization), so the specific requirements for destabilizing the higher-n harmonics seen in the HFS cases is unclear. But, we see here that the poloidal location of the massive gas jet can have a substantial enough effect on the spectrum of modes that are destabilized to change the confinement of REs during the TQ.

Figure 6:. Field lines at 0.4 ms for a LFS and HFS injection case, showing the importance of higher n harmonics for flux surface destruction.

IV. Summary

Considerable progress has been made in each of the two major topics..   The 2013 Theory Target is concerned with predicting disruption forces and runaway electron confinement.   The progress made in predicting disruption forces has been made possible by our ability to use the massively parallel computer Hopper at NERSC.   This allowed us to increase the total number of mesh points in our calculation by a factor of 8.   This higher resolution, and our continuing better understanding of the role of different physical parameters in producing disruption forces has allowed a much more realistic disruption simulation to be performed.

In the area of runaway electron confinement, the work presented here extends that described in the Q3 milestone report, primarily by presenting a more detailed analysis of the mode structure for different injection configurations.   This analysis allows a better understanding of present and future experiments and will lead to projections to ITER with greater reliability.

References:

[1] H. R. Strauss, R. Paccagnella, J. Breslau, ``Wall forces produced during ITER disruptions," Phys. Plasmas **17**, 082505 (2010).

[2] H. Strauss, R. Paccagnella, J. Breslau, L. Sugiyama, S. Jardin, "Sideways wall force produced during tokamak disruptions", Nuclear Fusion 53, 073018 (2013)

[3] H. Strauss, L. Sugiyama, R. Paccagnella, J. Breslau, S. Jardin, "Tokamak Toroidal Rotation caused by Disruptions," *to be submitted* (2013).

Acknowledgements:

Appendix: FY 2013 Theory Target on Disruption Physics:

Carry out advanced simulations to address two of the most problematic consequences of major disruptions in tokamaks: the generation and subsequent loss of high-energy electrons (runaway electrons), which can damage the first wall, and the generation of large electromagnetic loads induced by disruptions, and assess the severity of these effects on ITER

Original Quarterly Milestones:

Q1. Perform a 3D MHD simulation of a vertical displacement event (VDE) disruption at twice the resolution and wall time constant of previous studies to determine the scaling of the 3D forces on the axisymmetric conducting structures, and how these forces differ from those obtained in 2D calculations.

Q2. Perform a 3D MHD simulation of a DIII-D mitigated disruption experiment with symmetric impurity source terms to determine the effects of the source terms and MHD activity on test-particle runaway electron confinement.

Q3. Extend the 3D MHD simulations of VDEs to higher resolution by again doubling the grid resolution and increasing the simulation time period from that used in Q1. This will allow an increase in the Lundquist number to $S=10^6$ and a further doubling of the wall time-constant.

Q4. Extend the simulations of the DIII-D mitigated disruptions to model the effect of spatially non-symmetric source terms on runaway electron confinement.